

PAPER • OPEN ACCESS

Collection Grid Optimization of a Floating Offshore Wind Farm Using Particle Swarm Theory

To cite this article: Markus Lerch *et al* 2019 *J. Phys.: Conf. Ser.* **1356** 012012

View the [article online](#) for updates and enhancements.



IOP | ebooks™

Bringing you innovative digital publishing with leading voices to create your essential collection of books in STEM research.

Start exploring the **collection** - download the first chapter of every title for free.

Collection Grid Optimization of a Floating Offshore Wind Farm Using Particle Swarm Theory

Markus Lerch¹, Mikel De-Prada-Gil¹ and Climent Molins²

¹ Catalonia Institute for Energy Research (IREC), Jardins de les Dones de Negre 1, 2a pl., 08930 Sant Adrià de Besòs, Barcelona, Spain

² Universitat Politècnica de Catalunya (UPC), Department of Civil and Environmental Engineering, Jordi Girona 1-3, 08034 Barcelona, Spain

E-mail: mlerch@irec.cat

Abstract. Floating substructures for offshore wind turbines is a promising solution in order to harness the vast wind potential of deep water sites where bottom-fixed turbines are not feasible. The electrical system of large scale floating offshore wind farms will experience the application of new technologies and installation procedures that likely affect the cost-competitiveness. Thus, in this work, an optimization model based on the particle swarm theory is presented that allows optimizing the collection grid of a floating offshore wind farm. The developed model is applied to a study case consisting of a 500MW floating offshore wind farm located at the Golfe de Fos in the Mediterranean Sea. The resulting layout allows to reduce the total cost of the collection grid by more than 6% and to decrease the energy losses by 8% compared to the actual layout. Besides this, a further study analyzes the effect of a quantity discount with a reduced number of power cable cross sections.

1. Introduction

Offshore wind has become a significant source of power supply in Europe and is expected to expand worldwide [1]. However, most of today's offshore wind farms use bottom-fixed substructures that limit their feasible application to shallow water depths. Floating substructures for offshore wind turbines are a promising solution that enables to harness the abundant wind resources of deep waters [2]. As several floating offshore wind turbine (FOWT) concepts have been successfully tested in wave tanks and prototypes have been proven in open seas, floating offshore wind (FOW) is now reaching a pre-commercial phase where the first multi-unit FOW farms are being constructed in European waters [3]. Recently, WindEurope has outlined in its policy blueprint [4] the large potential of FOW and the ability to reach a levelized cost of energy of about 40€/MWh to 60€/MWh for commercial FOW farms by 2030. However, this is only achievable by significant cost reductions along the whole supply chain. The cost of the electrical system of bottom-fixed offshore wind farms can take up to 15% to 30% of the total investment in which the cost of cables takes a large portion [5]. For FOW farms the costs might be even higher since new technologies and installations procedures are applied. For instance, dynamic power cables are used instead of static cables due to the movement of the structure. Dynamic cables are especially designed with greater levels of armoring to cope with the torsion and tension exerted by the floating substructure and the mechanical stresses and friction appearing at the touchdown point on the seabed [6].



Content from this work may be used under the terms of the [Creative Commons Attribution 3.0 licence](https://creativecommons.org/licenses/by/3.0/). Any further distribution of this work must maintain attribution to the author(s) and the title of the work, journal citation and DOI.

Additional components may also be required such as buoyancy modules, bend stiffeners and joints. Besides the increased load on the cable, new procedures need to be tested for the hook-up and installation of the cables applied to FOWTs. Moreover, commercial scale FOW farms will likely include wind turbines with power ratings ranging from 6MW to 10MW or more, which require dynamic power cables with higher voltage levels. Hence, it is desirable to optimize the cable connection layout to obtain the most cost-effective solution. Existing studies have addressed mainly the optimization of the electrical layout of bottom-fixed offshore wind farms by using deterministic methods [7–10]. For instance, Banzo et al. optimized the electrical layout by using mixed integer quadratic programming [7]. The investment costs of the cables have been considered as well as the power losses. However, simplifications have been made to reduce the complexity of the problem by limiting the connection possibilities of each turbine to 1 and reducing the connections to the offshore substation. Besides that, 5 wind speed scenarios have been included and no change in wind direction [7]. The objective of this paper is to approach the complex problem of optimizing the inter-array cable collection grid of a FOW farm by applying the meta-heuristic particle swarm optimization model. The complexity is increased by considering a large range of wind speed and wind direction scenarios and taking into account the entire wind turbine connection possibilities. Besides that, a comprehensive wake model is included. Furthermore, dynamic power cables used for the connection of FOWTs are considered as well as their respective acquisition and installation costs. The paper is organized as follows. Section 2 explains the methodology and the model used for the optimization. Section 3 presents the application cases of the model and the conclusions of the paper are given in Section 4.

2. Methodology

2.1. Particle swarm optimization algorithm

The particle swarm optimization (PSO) is a population-based meta-heuristic optimization algorithm that was chosen due to its simplicity and high computational efficiency in solving non-linear complex problems [11]. In PSO, a possible solution is defined as a particle and is randomly initialized at the beginning. Each particle has its own position vector $x_j = (x_{j1}, x_{j2}, \dots, x_{jd})$ and velocity vector $v_j = (v_{j1}, v_{j2}, \dots, v_{jd})$, where j refers to the number of particles and d to the amount of dimensions [12]. A set of particles is called population and moves around in a multi-dimensional search space. The velocity and position of the particles are updated every iteration k according to Equations 1 and 2 in order to move the particles through the search space to find new and better solutions. Similar to how a bird of a swarm reconfigures its behavior based on its own experience and the experience of the rest of the birds, each particle updates its position based on its personal best solution $Pbest$ found so far, the global best solution $Gbest$ found by all particles and according to its velocity of the subsequent iteration v_j^{k+1} [12].

$$v_j^{k+1} = w^k * v_j^k + c_1 * r_1 * (Pbest_j^k - x_j^k) + c_2 * r_2 * (Gbest_j^k - x_j^k) \quad (1)$$

$$x_j^{k+1} = x_j^k + v_j^{k+1} \quad (2)$$

w^k represents the inertia weight. c_1 and c_2 are positive constants and r_1 and r_2 are randomly distributed numbers in the range [0,1] [13]. The first term of Equation 1 is called inertia and ensures that the particle moves in its path and does not change too abruptly. The second represents the memory of a particle and ensures that it moves towards its personal best solution ($Pbest$). The last term includes the cooperation and attracts the particle to a global best solution ($Gbest$), which is the one found by all particles [12]. The inertia weight changes with the iterations and can be determined as follows

$$w^k = w_{\max} - \frac{w_{\max} - w_{\min}}{k_{\max}} * k, \quad (3)$$

where w_{max} and w_{min} are the maximum and minimum inertia coefficients and k_{max} represents the maximum number of iterations [14]. The PSO algorithm updates within an iteration loop the particles position, velocity and P_{best} as well as G_{best} until convergence is obtained or a maximum number of iterations is reached [15].

2.2. Model implementation

The optimization model, based on PSO theory, has been implemented using MATLAB programming language and has been adapted in order to solve the collection grid optimization problem of this paper. The algorithm is illustrated in Figure 1.

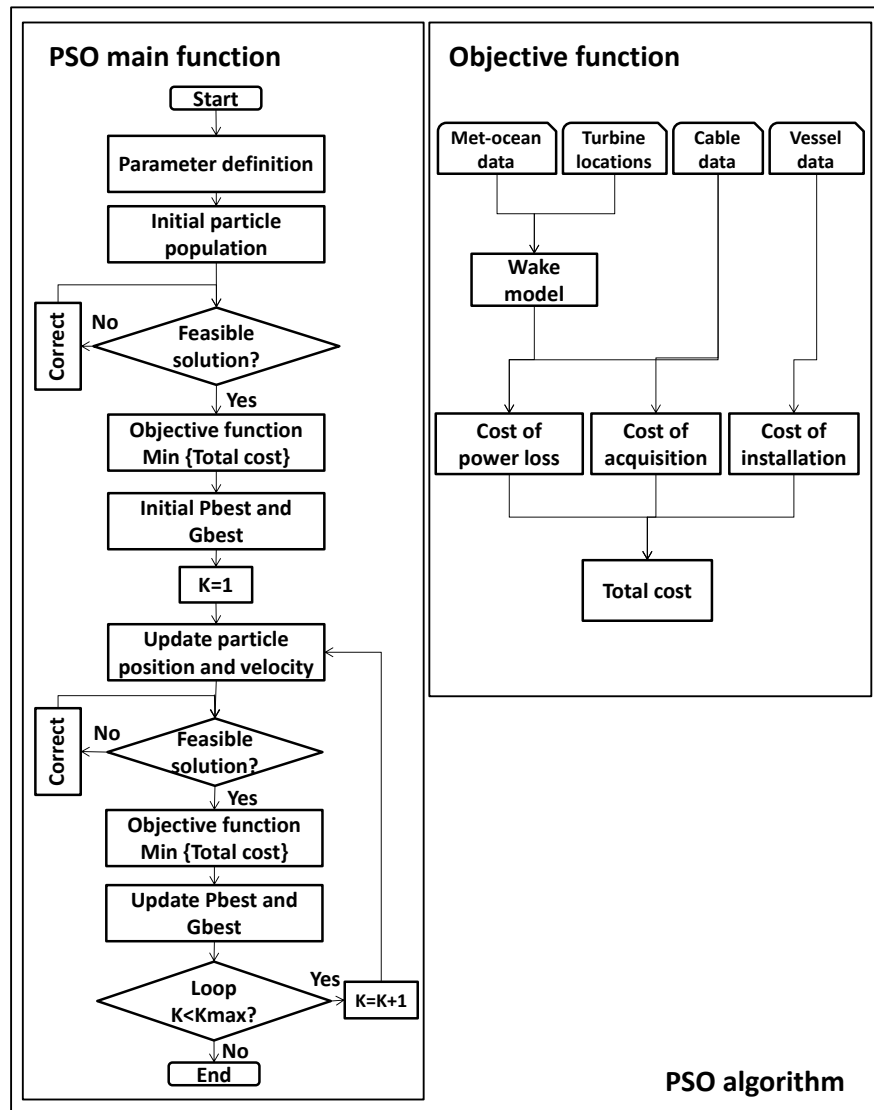


Figure 1: PSO algorithm applied.

The developed PSO model initializes with the definition of the main parameters and information about the wind farm layout such as the location of the wind turbines. Afterwards, an initial population is created consisting of particles with a three-dimensional position matrix.

$$x(a, 4, b), a \in \{1, 2, \dots, N_{wt}\}, b \in \{1, 2, \dots, j\}, \quad (4)$$

where N_{wt} is the number of FOWTs and j the number of particles. In the second dimension of the matrix four types of essential information are saved, which are represented by the parameter 4. This information includes the type of cable used for a connection, the two turbines connected by a cable and the power transmitted. After the initialization, each particle is checked if it provides a feasible solution to the problem by complying with a set of pre-defined constraints. In case a particle does not comply with a specific constraint, the model reallocates the connection of the FOWTs until the constraint is satisfied. Section 2.6 presents the constraints that are included in the optimization model. When the feasibility of all particles is ensured, the population is searched for the best solution. This can be mathematically described by the minimization of a function, called objective function. This subroutine computes the costs of each particle's solution and determines the one with the lowest total cost, which is then proposed as the initial $Pbest$ and $Gbest$. A more detailed description of the objective function is provided in Section 2.3. In the next step, the PSO algorithm updates the position and velocity of all particles according to Equations 1 and 2 and enters into a loop until a maximum number of iterations is reached. At each iteration the feasibility of the particles is checked as well as $Pbest$ and $Gbest$ updated by using the objective function.

2.3. Optimization problem

The objective is to minimize the cost of the collection grid considering the cost of acquisition $C_{acquisition}$, the installation cost $C_{installation}$ as well as the costs associated to the energy losses in the cables C_{loss} . The optimization problem for a single particle is defined as

$$\min(C_{acquisition} + C_{installation} + C_{loss}). \quad (5)$$

The acquisition cost takes into account the initial investment cost for the inter-array and export power cables. Furthermore, amortization is included considering the expected lifetime T of the FOW farm as follows

$$C_{acquisition} = \left(\sum_1^{N_{iac}} C_{iac} * L_{iac} + \sum_1^{N_{exc}} C_{exc} * L_{exc} \right) * \left(T \frac{i(1+i)^T}{(1+i)^T - 1} \right), \quad (6)$$

where C_{iac} represents the cost per meter of the inter-array cables and L_{iac} the length of the cables used to connect between the FOW turbines and the offshore substation. Likewise, C_{exc} defines the cost of the export cable and L_{exc} the length of the export cable. The number of inter-array and export cables are defined by N_{iac} and N_{exc} , respectively. The interest rate used for the calculation of the amortization is defined by i . The length of dynamic cable used for the interconnection of the turbines can be approximated by

$$L_{iac} = 2 * D_w * 2.6 + D_{WTs}, \quad (7)$$

where D_w represents the water depth and D_{WTs} the distance between two FOWTs. The installation cost includes the cost for installing the power cables and is obtained as

$$C_{installation} = \left(\left(\sum_1^{N_{iac}} L_{iac} + \sum_1^{N_{exc}} L_{exc} \right) * C_{vessel} * r_{instal} \right) * \left(T \frac{i(1+i)^T}{(1+i)^T - 1} \right), \quad (8)$$

where C_{vessel} is the day rate of the cable laying vessel and r_{instal} represents the installation rate in days per meter. The cost associated to the energy losses in the cables can be determined by

$$C_{loss} = \sum_{v_{min}}^{v_{max}} \sum_{0^\circ}^{360^\circ} \left(\left(\sum_1^{N_{iac}} Ploss_{iac} + \sum_1^{N_{exc}} Ploss_{exc} \right) * H_{ws} * H_{wd} * T \right) * C_{energy}, \quad (9)$$

where $P_{loss_{iac}}$ and $P_{loss_{exc}}$ are the power losses in the inter-array and export cables, respectively. N_{iac} and N_{exc} are the number of inter-array and export cables. Wind speed and wind direction are included as stochastic variables. The occurrence probabilities of wind speed and wind direction are defined by H_{ws} and H_{wd} , respectively. The total cost of energy losses are obtained as the sum of energy losses according to different wind speeds and wind directions and multiplied by the cost per unit of energy C_{energy} .

2.4. Power loss computation

The power generated by a wind turbine can be calculated as follows

$$P_{gen} = \frac{1}{2} \rho_a A_{rotor} C_p(\lambda, \beta) v_{ws}^3, \quad (10)$$

where A_{rotor} accounts for the rotor swept area and ρ_a for the density of air. C_p is the power coefficient and v_{wind} represents the wind speed at hub height. The power coefficient depends on the blade tip-speed ratio λ and the blade pitch angle β [16]. The power loss in any power cable of the FOW farm can be determined by

$$P_{loss} = 3 \left(\frac{P_{gen} + P_{trans}}{\sqrt{3} * U} \right)^2 * R_{cable} * L_{cable}, \quad (11)$$

where P_{gen} is the power generated by the FOWT from which the cables exists. P_{trans} represents the power that has been transmitted to this FOWT from another wind turbine. U is the voltage applied, for example, medium voltage for inter-array cables and high voltage for the export cable. The resistance of the power cable is represented by R_{cable} and L_{cable} defines the length of the cable.

2.5. Wake model

A comprehensive wake model has been included in the optimization model to calculate the wind speed v_{ws} for the power generation calculation at each FOWT. The wake model has been developed previously by Mikel De-Prada-Gil and has been applied for instance as part of a control strategy to maximize the energy yield of offshore wind farms [17]. The model considers single, partial and multiple wake effects among turbines. Besides that, it takes into account the wind direction of the free-stream wind speed. It is based on the wake concept developed by Jensen [18]. Furthermore, global momentum conservation in the wake downstream of the wind turbine is considered as well as a linear expansion of the wake downstream. However, turbulent behavior caused by wakes is neglected. A detailed description of the model is provided in [19]. For the sake of completeness, an outline of the methodology is presented next.

- Single wake:

The downstream wind speed of a single turbine is described as

$$v_2 = v_1 \left[1 - \left(\frac{D_{rotor}}{D_{rotor} + 2 * k_{wake} * x} \right)^2 * (1 - \sqrt{1 - C_t}) \right], \quad (12)$$

where v_2 is the wind speed at distance x from the FOWT, D_{rotor} is the diameter of the turbine rotor, C_t is the thrust coefficient, v_1 is the free-stream wind and k_{wake} is the wake decay constant [18].

- Partial wake:

Partial wake is a phenomenon which occurs when one or more wind turbines cast a single shadow on a downstream turbine. The wind speed entering into the turbine m affected by the upstream wind turbine n is then given by [20]

$$v_m = v_1 \left(1 - \sqrt{\sum_{n=1}^N \beta_{T_m, T_n} * \left(1 - \frac{v_{T_n}}{v_1} \right)} \right), \quad (13)$$

where v_m is the wind speed of the downstream turbine m , v_1 is the initial wind speed entering into the wind turbine n , v_{T_n} is the shadow of n falling on the m th wind turbine and β_{T_m, T_n} is the ratio of the shadow area by the wake to the total rotor area.

- **Multiple wakes:**

In a wind farm with a large number of turbines, a single wind turbine can be affected by several wakes. The multiple wake model takes this effect into account. It assumes that the kinetic energy deficit of interacting wakes is equal to the sum of the energy deficits of the individual wakes [19]. Thus, the velocity at the intersection of several wakes can be determined by [21]

$$1 - \frac{v_x}{v_1} = \sqrt{\sum_{n=1}^N \left(1 - \frac{v_n}{v_1} \right)^2}, \quad (14)$$

where v_1 is the initial free-stream velocity, N is the total number of upstream influencing turbines, v_n is the wind speed affected by the individual wake n and v_x is the wind speed such that all the wakes are taken into account [17].

2.6. Constraints

The optimization model includes several constraints that have to be satisfied by all particles in order to count as a suitable solution.

- The energy leaving a turbine must be supported by a single cable.
- A maximum of one cable can be placed between two turbines.
- The crossing of power cables is not allowed.
- The building of a ring connection is not allowed. A ring is a connection between several FOWTs that does not end in a connection to the offshore substation.
- The power transmitted by a cable cannot exceed the capacity of the installed cable.

3. Application

3.1. Study case

A 500MW FOW farm has been considered as a study case for the application of the optimization model. It consists of 50 FOWTs with each having a rated power capacity of 10MW. The DTU 10-MW reference wind turbine has been considered and related specifications are given in [22]. Golfe de Fos has been chosen as offshore site. It is located in the south of France in the Mediterranean Sea. The reference water depth is about 70m and the environmental conditions are moderate. The wind rose of the offshore site is presented in Figure 2 and shows how wind speed and wind direction are distributed at the location. More information about the offshore site is provided in [23]. The collection grid of the FOW farm is operated at 66kV and the transmission voltage is 220kV. Dynamic power cables are used for the connection of the FOWTs. Figure 3 presents the FOW farm and the actual collection grid layout. The FOWTs are placed in direction to the prevailing winds. The offshore substation is located to the east of the FOW farm. The present layout is based on work performed in the LIFES50+ project [24], but has not been subject to an optimization. Hence, the objective of this paper is the optimize it. Table 1 presents the costs and power losses of the actual electrical grid layout.

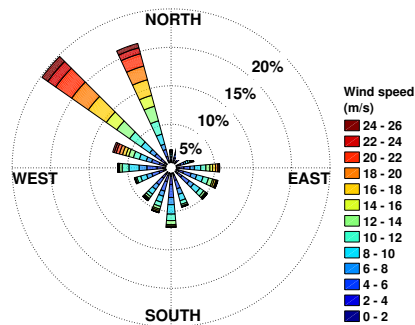


Figure 2: Wind speed and wind direction distribution at Golfe de Fos.

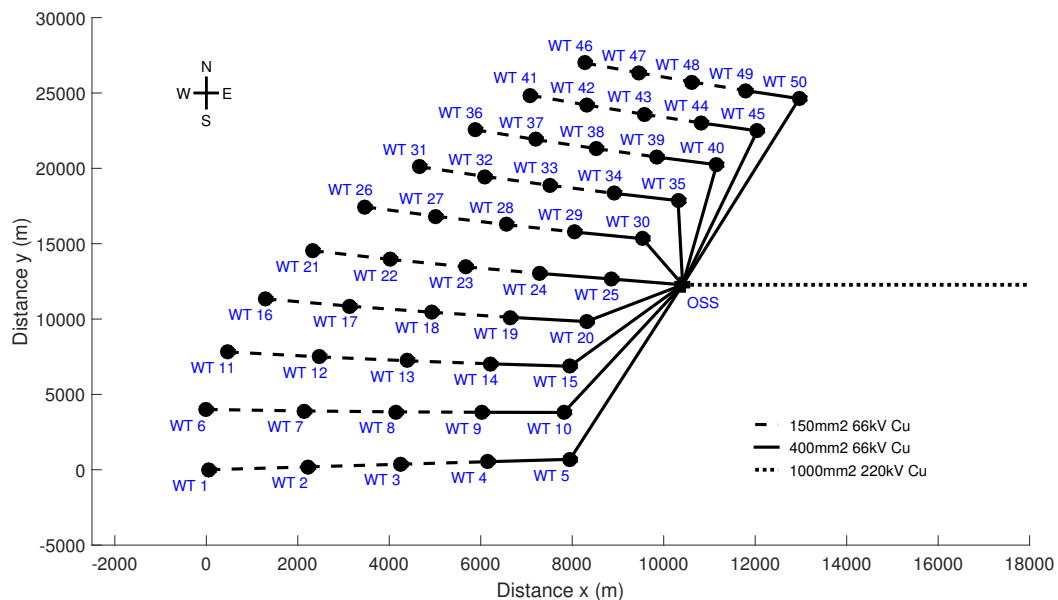


Figure 3: Golfe de Fos actual layout.

Table 1: Cost and power losses of actual layout.

	Inter-array cables	Export cables	Total
Acquisition cost $C_{\text{aquisition}}$ (M€)	91.92	69.09	161.01
Installation cost $C_{\text{installation}}$ (M€)	19.71	8.12	27.83
Cost of energy loss C_{loss} (M€)	27.38	3.34	30.72
Total cost C_{total} (M€)	139.01	80.55	219.56
Annual energy loss E_{loss} (MWh)	17112.55	2086.85	19199.10
Total length of cables L_{cable} (km)	155.73	64.20	219.93

The costs and losses are based on the following input data. A lifetime of 20 years is considered and an interest rate of 4%. The cost per unit of energy is assumed at 80€/MWh. Two export cables are used for the transmission of the power to the onshore substation. The distance from the offshore substation to shore is 32.1km. Information regarding the power cables is displayed in Table 2. This data is based on assumptions and should be considered only as an example for the purpose of this study.

Table 2: Power cable data.

	Inter-array						Export
Cross section (mm ²)	95	150	300	400	630	800	1000
Resistance (Ω /km)	0.25	0.158	0.078	0.059	0.037	0.029	0.0243
Unit cost (€/m)	220	300	423	475	554	683	740
Power capacity (MW)	26	31	44	51	62	71	269

3.2. Optimization results

The developed PSO model is applied on the Golfe de Fos FOW farm case. The number of particles is set to 10 and a total of 20 iterations is considered. The FOWT connection layout obtained from the optimization is presented in Figure 4.

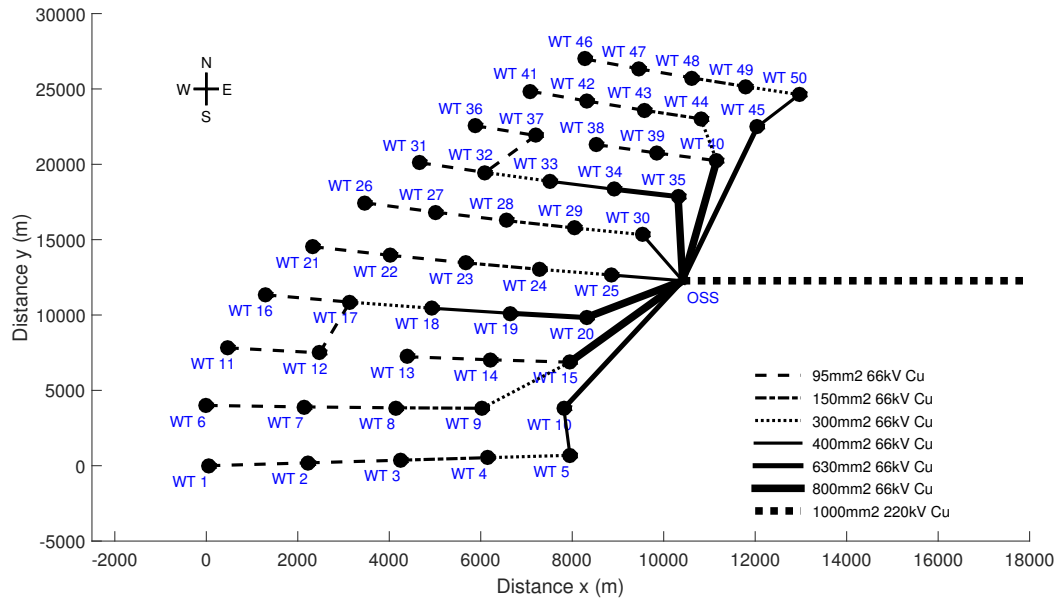


Figure 4: Collection grid layout optimized.

The new layout is similar but some changes are observable. For instance, the number of FOWTs connected to the offshore substation has decreased from 10 to 8. Furthermore, there exist strings of a higher number of FOWTs than before. For example, a string of 7 FOWTs exists that requires the use of inter-array cables with larger cross sections up to 800mm². Table 3 presents the costs and energy losses for this collection grid layout.

Table 3: Cost and power losses of optimized layout.

	Inter-array cables	Export cables	Total
Acquisition cost $C_{\text{acquisition}}$ (M€)	86.34	69.09	155.43
Installation cost $C_{\text{installation}}$ (M€)	18.06	8.12	26.18
Cost of energy loss C_{loss} (M€)	25.15	3.34	28.49
Total cost C_{total} (M€)	129.55	80.55	210.10
Annual energy loss E_{loss} (MWh)	15716.00	2086.85	17802.85
Total length of cables L_{cable} (km)	142.73	64.20	206.93

In comparison to Table 1, it can be seen that the total cost of the inter-array cables has decreased by more than 6% and the energy losses by 8% despite the use of larger cross sections. This is mainly due to the decrease in the total length of the cables since fewer cables are used and less connections to the offshore substation exist.

3.3. Reduced power cable type usage

In the wind industry it is quite common that a supplier of power cables provides a discount on the purchase of a large amount of cables. Developers often prefer to use less different cables and apply larger cross sections for each of the wind turbines in the farm. Hence, it is of interest to analyze the effect of such a discount. Therefore, based on the layout obtained from the previous optimization, the number of available power cables is reduced to the 2 largest cross sections (630mm^2 and 800mm^2) and a discount of 15% on the price is applied. Figure 5 shows the comparison of the results for the inter-array cables and the total cost.

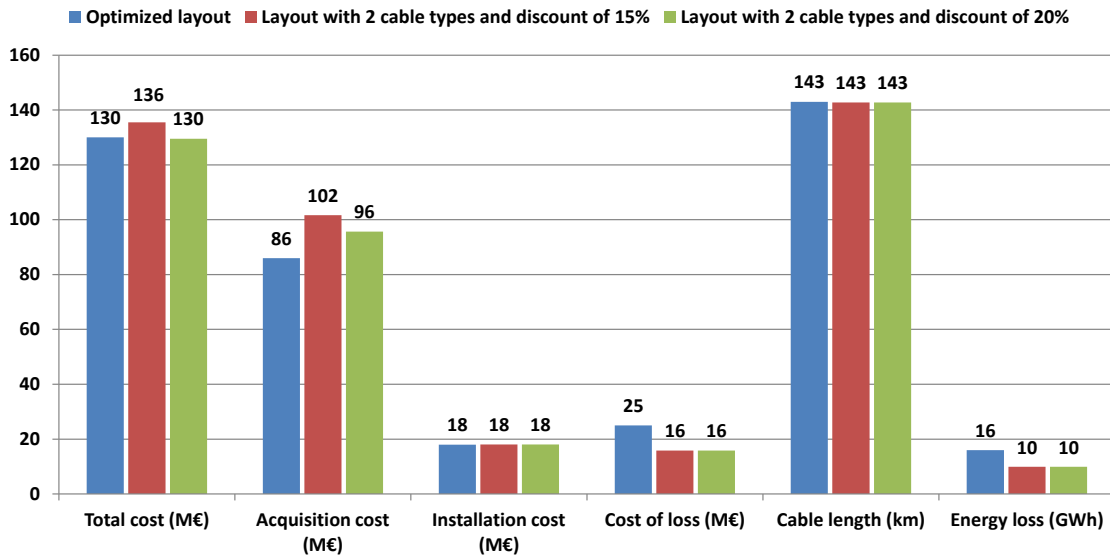


Figure 5: Comparison of inter-array costs and energy losses for quantity discount

It is observable that despite the discount of 15%, the acquisition cost of the inter-array cables is higher since more cables with larger cross sections and higher unit costs are used. However, the use of solely larger cross sections allows to reduce the energy losses and the cost of energy loss. Nevertheless, the total cost of the collection grid is higher for the layout considering the quantity discount. This allows to conclude that the applied discount on the power cables is not sufficient to compensate the primary use of cables with larger cross sections.

A sensitivity analysis of different discount rates has found that a discount of at least 20% is required to equal the total cost. The results obtained for this discount rate are shown in green in Figure 5 for the sake of completeness.

4. Conclusion

In this paper, an optimization model is presented based on particle swarm theory. The model has been adapted to solve the optimization problem of the electrical collection grid of a floating offshore wind farm. An application case consisting of a 500MW floating offshore wind farm with fifty 10MW wind turbines has been considered. The floating offshore wind farm is placed at the Golfe de Fos site in France. The optimization study results in a layout using fewer cables but with larger cross sections and a few modifications in the connections. This allows to reduce the total cost of the collection grid by more than 6% and the energy losses of the inter-array cables by 8%. The total length of the required cables could also be reduced by more than 8%. A study on the application of a quantity discount of 15% and the use of solely large cross sections has demonstrated an unfavorable increase of the total costs of inter-array cables by more than 4%. A discount of at least 20% would be required to equal the total cost. Further research on this topic is planned and includes the consideration of different dynamic cable configurations such as the use of only dynamic cables or the use of a combination of static and dynamic cables. Besides that, the use of central hubs for the connection of the FOWTs could be considered as well as an optimization of the location of the offshore substation. Reliability of the system components and respective energy losses could also be taken into account.

Acknowledgements

This work was supported by the European Union Horizon 2020 program under the grant agreement H2020-LCE-2014-1-640741.

References

- [1] GWEC 2018 URL <http://gwec.net/publications/global-wind-report-2/>. [Accessed October 18, 2018]
- [2] Rhodri J and Costa Ros M 2015 *Carbon Trust*
- [3] WindEurope 2017
- [4] WindEurope 2018
- [5] Ling-Ling H, Ning C, Hongyue Z and Yang F 2012 *IET*
- [6] Young D 2018 *ORE Catapult Technical Report*
- [7] Banzo M and Ramos A 2011 *IEEE Transactions on Power Systems*
- [8] Fischetti M and Pisinger D 2018 *Electronic Notes in Discrete Mathematics*
- [9] Pillai A, Chick J, Johanning L, Khorasanchi M and de Laleu V 2015 *Engineering Optimization*
- [10] Lumbreras S and Ramos A 2013 *IEEE Transactions on Power Systems*
- [11] Hou P, Hu W and Chen Z 2016 *IET Renewable Power Generation*
- [12] Dauer M, Meyer J, Jaeger J, Bopp T and Krebs R 2016 *Power Systems Computation Conference (PSCC)*
- [13] Abido M 2002 *International Journal of Electrical Power & Energy Systems*
- [14] Boubaker S, Djemai M, Manamanni N and M'sahli F 2014 *Applied Soft Computing*
- [15] Hou P, Hu W, Soltani M and Chen Z 2015 *IEEE Transactions on Sustainable Energy*
- [16] Bianchi F, de Battista H and Mantz R 2006 *Wind Turbine Control Systems: Principles, Modelling and Gain Scheduling Design*
- [17] De-Prada-Gil, M et al 2015 *Energy Conversion and Management*
- [18] Jensen N O 1983 *Risø National Laboratory Roskilde*
- [19] De-Prada-Gil M 2014 *Design, operation and control of novel electrical concepts for offshore wind power plants*
Ph.D. thesis Universitat Politècnica de Catalunya
- [20] Ali M, Matevosyan J, Milanović J and Söder L 2009 *8th International Workshop on Large Scale Integration of Wind Power*
- [21] Bie Z, Zou X, Wang Z and Wang X 2009 *Power & Energy Society General Meeting*
- [22] Bak, C et al 2013 *Danish Wind Power Research*
- [23] Gonzalez, P et al 2015 *Deliverable LIFES50+*
- [24] LIFES50+ 2015 URL <https://lifes50plus.eu>. [Accessed December 20, 2018]